Supernova 1987A:30 years later - Cosmic Rays and Nuclei from Supernovae and their aftermaths
Proceedings IAU Symposium No. 331, 2017
A. Marcowith, M. Renaud, G. Dubner, A. Ray & A. Bykov, eds.

doi:10.1017/S1743921317004811

Evidence for a wide electron spectra scatter among different SNR regions from high radio-frequency observations

A. Pellizzoni[1], E. Egron[1], M. N. Iacolina[1], S. Loru[1,2], M. Marongiu[1], S. Righini[3], M. Cardillo[4], A. Giuliani[5], S. Mulas[2], G. Murtas[2] and D. Simeone[2]

[1]INAF, Osservatorio Astronomico di Cagliari, Via della Scienza 5, 09047 Selargius, Italy

[2]Dip. di Fisica, Università degli Studi di Cagliari, SP Monserrato-Sestu, KM 0.7, 09042 Monserrato, Italy

[3]INAF, Istituto di Radio Astronomia di Bologna, Via P. Gobetti 101, 40129 Bologna, Italy

[4]INAF, Osservatorio Astrofisico di Arcetri, Largo E. Fermi 5, 50125 Firenze, Italy

[5]INAF, Istituto di Astrofisica Spaziale e Fisica cosmica di Milano, via E. Bassini 15, 20133 Milano, Italy

email: apellizz@oa-cagliari.inaf.it

Abstract. In the framework of the Sardinia Radio Telescope (SRT) Early Science Program, we obtained single-dish high-resolution imaging of the Supernova Remnants IC443 and W44 at 7 GHz. By coupling them with SRT 1.5 GHz maps, we provided spatially-resolved spectral measurements that are highlighting a spread in spectral slope distribution. The observed features range from flat or slightly inverted spectra corresponding to bright radio limbs and filaments, to relatively steep spectra in fainter radio regions. Different theoretical possibilities explaining the above challenging findings are discussed. In particular, we exclude that the observed region-dependent wide spread in spectral slope distribution could be related to absorption processes. Our high-frequency results can be directly related to distinct electron populations in the SNRs including secondary hadronic electrons and resulting from different shocks conditions and/or undergoing different cooling processes. Integrated fluxes associated with the whole SNRs obtained by SRT in comparison with previous results in the literature support the evidence for a slight spectral steepening above 1 GHz for both sources, which could be related to primary electrons or more likely secondary hadronic electrons cut-offs.

Keywords. ISM: supernova remnants – ISM: individual objects: W44, IC443 – radio continuum: ISM

1. Introduction

Despite the growing interest in high-energy GeV−TeV emission and its connection with radio emission, multi-wavelength data of SNRs are sparse and often missing. Synchrotron radio emission is expected at least up to $20-50$ GHz, and is produced by electrons with energies in the GeV range and magnetic fields of $> 10-100$ μG. However, for the most interesting and bright objects, high-resolution images at frequencies >5 GHz in the confused regions of the Galactic Plane are lacking and not easily achievable through interferometry due to the very large SNR structures.

Integrated fluxes are typically available in the literature for up to $5-10$ GHz, while SNR spatially-resolved fluxes are largely unexplored in this frequency range and above. In particular, a better characterisation of radio spectra (synchrotron spectral indices

and breaks) is necessary for constraining the high-energy spectra in the frame of IC/bremmstrahlung leptonic models and probe them versus hadronic models. For example, the gamma-ray fluxes and spectra are strongly dependent on the IC photon target parameters and spectral breaks in the electron distribution, and in most cases there are no unambiguous model solutions without detailed measurements of the latter, since the former is intrinsically uncertain (Cardillo *et al.*, 2014; Ackermann *et al.*, 2013; Giuliani *et al.*, 2011). Furthermore, a careful verification (through single-dish imaging, possibly in combination with interferometric data) of co-spatiality of the radio high-frequency and gamma-ray emissions could provide a crucial test of the hypothesis of hadron vs. electron emission. In fact, recent constraints on cosmic ray emission from SNRs and related models (e.g. Ackermann *et al.*, 2013) are based on integrated radio fluxes only (no spatially resolved spectra), implying the simplistic assumption of a single electron population for the whole SNR.

SNR IC443 and W44 represent ideal targets for better testing the above models, thanks to their interesting complex morphology and availability of extensive multi-wavelength data, from radio to gamma rays.

We focused on the need for spectral imaging of IC443 and W44 with good angular resolution and sensitivity at high-radio frequencies obtained by the recently commissioned Sardinia Radio Telescope (SRT; *www.srt.inaf.it*).

2. Integrated and spatially-resolved radio spectra of SNR IC443 and W44

Single-dish radio mapping with SRT of IC443 and W44 at L (1.55 GHz, HPBW 11.1') and C-band (7 GHz, HPBW 2.71') is described by Egron *et al.* (these proceedings).

Comprehensive spatially-resolved spectra were determined by combining C-band and L-band maps produced with the same parameters and topology (same projection centre and pixel size). In particular, spectral index maps were obtained by convolving data at low resolution (accordingly to L-band resolution). The corresponding images are reported in Fig. 1 and 2 for IC443 and W44, respectively, together with the surface brightness maps of the sources in C-band. Since on-the-fly single-dish imaging techniques allow us precise measurements of the density flux for each direction in the sky (i.e. for each pixel map), the spectral index estimate is directly obtained fitting the two L-band and C-band measurements for each pixel. Single-dish flux measurements are straightforward with respect to the more complex interferometric data processing, and related errors are typically lower (conservatively, about 3% in L-band). On the other hand, the available angular resolution for low-frequency single-dish imaging is much worse than that from interferometric images. Our first low-resolution result for single-dish spectral mapping of SNRs gives us an estimate of region-dependent spectral indices and a direct correlation with the corresponding brightness of the largest sub-regions targets (small structures are missing in our spectral index maps). More accurate (i.e. higher angular resolution) images could be provided for example through combination of C-band and K-band (22 GHz) images, the latter having about 40" HPBW (see Loru *et al.*, these proceedings).

For both sources we observed a significant spread in the distribution of the spatially-resolved spectra ranging from a flat (for W44) or slightly inverted (up to -0.5 for IC443) spectral index to a relatively steep spectrum (α>0.7) compared to a mean value of $\sim$0.5 (where the flux density is $S \propto \nu^{-\alpha}$). Relative errors among adjacent pixels are <1%. Our data highlight a correlation between the brightest flux density regions and flat spectral indices for IC443 and W44. These regions are mainly located on the edge and on the brightest filaments of the SNRs. They match with the bulk of the gamma-ray emission

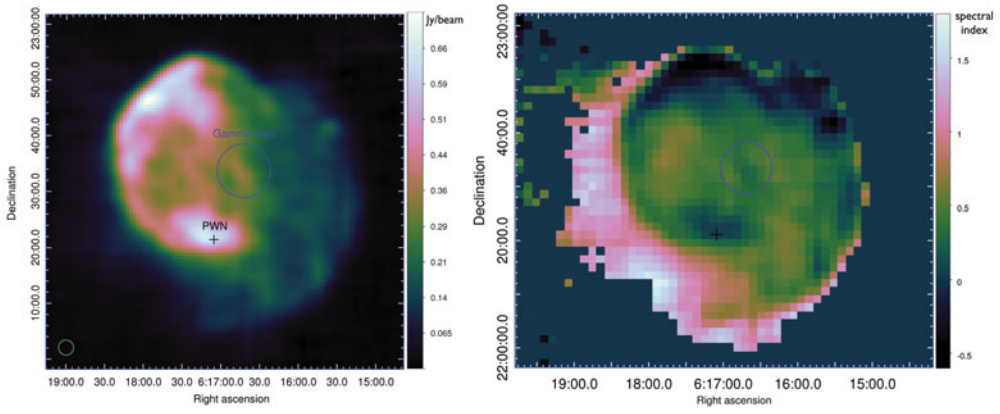

Figure 1. Continuum map of SNR IC443 at 7 GHz (left) and a preliminary spectral index map obtained by using 1.55 and 7 GHz data (right). The plus simbol indicates the position of the PWN powered by the neutron star CXOU J061705.3+222127, whereas the circle indicates the bulk of the gamma-ray emission seen with VERITAS (see text).

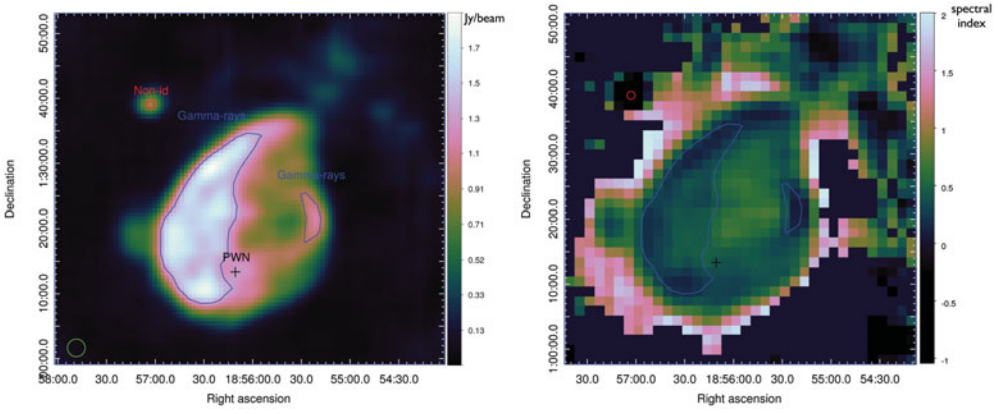

Figure 2. Continuum map of SNR W44 at 7 GHz (left) and a preliminary spectral index map obtained by using 1.55 and 7 GHz data (right). The cross and the circle indicate the position of the PWN powered by the pulsar PSR B1853+01 and a bright point-like source, respectively. The highlighted areas correspond to the gamma-ray emissions detected with AGILE and Fermi-LAT (see text).

in the case of W44. The approximate location of the gamma-ray emission detected with VERITAS and Fermi-LAT for IC443 (Humensky *et al.*, 2015), and with AGILE (Giuliani *et al.*, 2011) and Fermi-LAT in the case of W44 (Abdo *et al.*, 2010), was indicated in the Fig. 1 and 2.

Our measurements for IC443 provided integrated flux densities of $S_{1.55\mathrm{GHz}} = 133.7 \pm 4.0$ Jy and $S_{7\mathrm{GHz}} = 66.8 \pm 2.9$ Jy. For W44 we obtained $S_{1.55\mathrm{GHz}} = 214.4 \pm 6.4$ Jy and $S_{7\mathrm{GHz}} = 93.7 \pm 4.0$ Jy (see Egron *et al.*, these proceedings). It is worth noting that typical continuum flux errors for these sources in the literature are of the order of $\sim 10 - 15\%$, while we provided more accurate measurements. This is mostly due to our oversampled maps in which, for each pixel, tens of OTF baseline-subtracted scans are available, providing straightforward error measurements through standard deviation estimates.

From a weighted fit of the SRT data, our spectral index estimate for IC443 in the interval $1.55 - 7.2$ GHz is $\alpha = 0.46 \pm 0.03$. This result is in perfect agreement with a spectral index estimate of $\alpha = 0.47 \pm 0.06$ obtained through a weighted fit of all previous

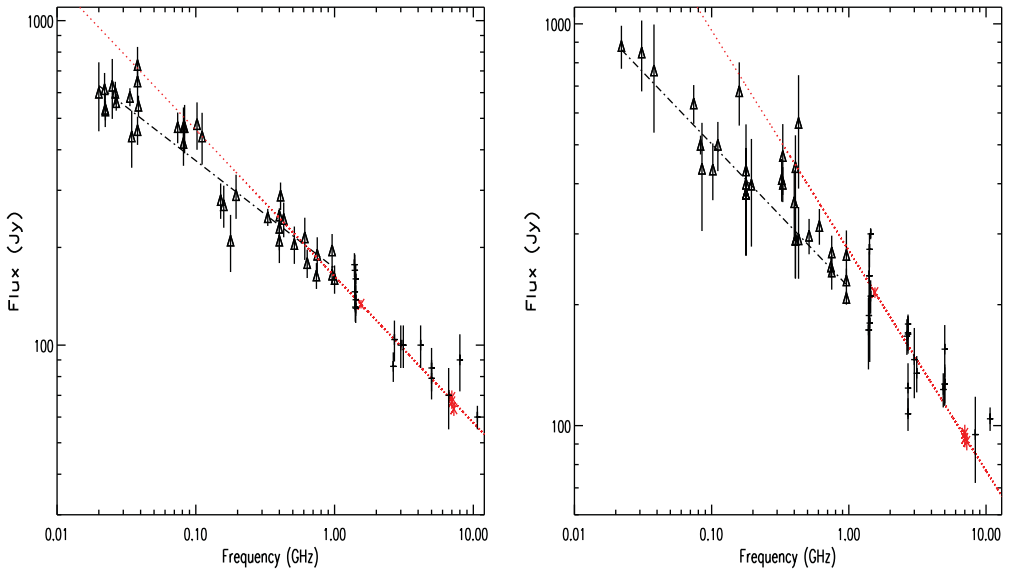

(a) IC443 (b) W44

Figure 3. Integrated radio continuum spectra of IC443 (a) and W44 (b) obtained from the flux density values (black points) listed in Castelletti *et al.*, 2011 and Castelletti *et al.*, 2007, and SRT measurements (asterisks). The spectral indices derived from SRT data at high frequencies ($1.5-7.2$ GHz) are steeper (dotted line) than that obtained from lower frequency measurements ($0.02-1$ GHz; triangles, dot-dashed line fits). These possible spectral turn-offs around $\sim$1 GHz were not evident from the large spread in previous measurements, in particular at high frequencies.

radio data available in the literature considering the frequency range $1.39-8.0$ GHz (see Table 2 in Castelletti *et al.*, 2011 for a direct comparison). Focusing the same analysis on the literature data at low frequencies ($0.02-1.0$ GHz), we obtain that the IC443 spectrum flattens to $\alpha = 0.33 \pm 0.01$. Thus, a slight steepening of the IC443 spectrum ($\Delta\alpha \sim 0.1$) around $\sim$1 GHz is suggested considering previous literature data (though not statistically significant: $\sim 2\sigma$ level) and is now confirmed at $> 4\sigma$ confidence level by SRT observations (see Fig. 3).

W44 displays a similar spectral behaviour as compared to IC443. In fact, the high-frequency spectral index estimated by SRT for W44 is $\alpha = 0.55 \pm 0.03$ ($1.55-7.2$ GHz). Looking at low-frequency flux measurements reported in Table 2 of Castelletti *et al.* (2007), the resulting spectral index is significantly softer (see Fig. 3). A weighted fit to the data in the $0.02-1.0$ GHz range gives a spectral index $\alpha = 0.36 \pm 0.02$ associated with a very significant goodness-of-fit (reduced $\chi^2 = 1.06$). Thus, even for W44, SRT data suggest a spectral steepenening at high frequencies, which could be related to the approach to a possible break in electron energy distribution (as averaged for the whole SNR extent). It is possibly associated with cooling processes and/or intrinsic particle distribution features at the shock.

A typical primary particle spectrum (both hadronic and leptonic) is expected to have a high energy cut-off which depends on the SNR age and other physical parameters (i.e. ambient density and magnetic field). In fact, gamma-ray observations pointed out a steepening of the primary particle spectrum at energies of $\sim$ 10 GeV for W44 and $\sim$ 100 GeV for IC443 (Cardillo *et al.*, 2014; Ackermann *et al.*, 2013; Giuliani *et al.*, 2011) that implies synchrotron break/cut-off at frequencies >10 GHz. However, a secondary

electron population produced by hadronic interactions could represent a major fraction of the whole leptonic plasma present in the SNR (Cardillo *et al.*, 2016; Lee *et al.*, 2015). These secondary hadronic electrons are expected to take $\sim 10\%$ of the primary particle energy. Thus, a corresponding synchrotron spectrum change due to this particle population could be expected in the GHz range, in addition to the primary particle spectrum change at higher frequencies.

In order to properly investigate the actual parameters of region-dependent electron distributions, spatially-resolved, high-frequency spectra must be considered.

We observe a significant spectral scatter along different SNR regions in our data. The simplistic assumption of a single-electron population approximation, typically postulated in SNR physical modelling, seems manifestly hindered. For both IC443 and W44, SRT images demonstrate that flat spectra correlate with the brightest SNR regions near the limbs or filaments, while the fainter central regions and halos display steeper spectra. Spectral flattening corresponding to bright regions of IC443 (e.g. toward the eastern boundary) was also evident from the analysis of VLA data at lower frequencies of $74-330$ MHz (Castelletti *et al.*, 2011), although in this case this effect was related to thermal absorption, unlikely working at higher frequencies.

The significant spread in spectral index distributions within different SNR regions observed by SRT could in principle be related to several and possibly concurring processes.

Thermal absorption (free-free) was invoked to explain (A) the low-frequency cut-offs ($<$50 MHz) observed in the integrated SNR spectrum of IC443, and (B) the apparent spread in spectral index distributions seen by the VLA at $<$1 GHz that is possibly correlated with the nonuniform optical depth along the SNR. The reported average free-free continuum optical depth derived for IC443 by Castelletti *et al.* (2011) is negligible for frequencies $>$ 50 MHz, but in principle absorption processes could be effective at higher frequencies if strong local enhancements of the optical depth are present. In fact, extrapolating the reported free-free optical depth local peaks for IC443 ($\tau_{74} \sim 0.3$ at 74 MHz) to $\nu > 1$ GHz, we obtain absorption coefficients $\exp(-\tau_{74}(\nu/74_{\rm MHz})^{-2.1}) \sim 1$. Thus, we can exclude that free-free thermal absorption could be responsible for the observed spectral index, region-dependent scatter at high frequencies.

The observed spread in the spectral index distribution of both IC443 and W44 could instead be related to an intrinsic variety in the primary and secondary electron spectra (spectral slopes and breaks) produced in shocks that are located in different SNR/PWN environments, -i.e. several region-dependent electron populations are present. Naive shock acceleration theory predicts a single particle spectrum that is a power law in momentum with spectral index $\sim$2, with little fluctuation depending on the actual shock parameters (e.g. Sturner *et al.*, 1997 and reference therein). The resulting synchrotron spectral slope is then expected to be $\sim$0.5, a value that is compatible with our integrated spectra above $\sim$1 GHz. On the other hand, standard models fail to predict flat or inverted spectra as seen in bright SNR selected regions. Even in the ultrarelativistic regime and assuming a high shock compression factor ($\sim$4), electron spectra slopes are expected to be above $\sim$1.5 (Ellison *et al.*, 1996; Ellison *et al.*, 1996), thus implying a synchrotron spectral index $>$0.2 that is incompatible with our results.

In order to overtake this incongruency, we note that a spectral flattening effect related to the contribution of secondary hadronic electrons could be present in addition to the primary electron canonical distribution (Cardillo *et al.*, 2016). In fact, the correlation among bright flat-spectrum SNR regions and gamma-ray emission could represent a possible signature of enhanced hadronic emission (and then significant secondary hadronic electrons injection). For W44, gamma-ray emission seems to be associated with the bright radio rims and filaments of the SNR (Cardillo *et al.*, 2014; Giuliani *et al.*, 2011; Abdo

et al., 2010). Instead, the IC443 gamma-ray emission seems to be anticorrelated with SNR limbs, although it is still associated with a relatively bright radio filament (with a flatter spectrum w.r.t. average central region spectra) close to a molecular cloud enhancing IC/bremsstrahlung emission (Humensky *et al.*, 2015). Thus, the observed spread in spectral slopes could in principle reflect a region-dependent amount of secondary electron production, however this hypothesis cannot be clearly proven by present multi-wavelength data.

On the other hand, spectral steepening could also be related to strongly-enhanced, region-dependent cooling. However, this hypothesis is disfavoured by the evidence for a correlation among bright flat-spectrum radio regions and gamma-ray emission (i.e. the electron cooling to gamma-ray energies does not significantly affect radio spectra). Furthermore, models of temporal evolution of nonthermal particle and photon spectra at different stages of shell-type SNR lifetime indicate that no significant steepening of the spectral index due to synchrotron cooling is expected from a particle gas drifting away from the shock region on a time-scale of $10^4 - 10^5$ yrs (Sturner *et al.*, 1997), unless a significant local enhancement of the magnetic field can be envisaged. However, both primary and secondary electron distribution cut-offs could approach the synchrotron radio-emitting range on these time-scales, thus providing a change in the synchrotron spectral index at high frequencies. In fact, as reported above, a slight steepening of the integrated spectra of both IC443 and W44 at frequencies >1 GHz is observed. Region-dependent spectral slopes could reflect the presence of different electron distribution cut-off energies. In order to assess spectral curvature and cut-offs, high-resolution spectral imaging at frequencies >10 GHz is required.

3. Summary

In the context of the early science observations with SRT, we obtained single-dish, high-resolution maps of SNR IC443 and W44 at 7 GHz, which provide accurate continuum flux density measurements (see Egron *et al.*, these proceedings). By coupling SRT 7 GHz maps with SRT 1.5 GHz maps, we obtained (low resolution) spatially-resolved spectral measurements that are suggesting a spread in spectral slope distribution, ranging from flat spectra corresponding to bright regions, to relatively steep spectra ($\alpha \sim 0.7$) in fainter radio structures of the SNRs.

We exclude that the observed region-dependent wide spread in spectral slope distribution could be associated to absorption processes. Our high-frequency findings can be directly related to distinct electron populations in the SNRs including secondary hadronic electrons and resulting from different shocks conditions and/or undergoing different cooling processes.

Integrated fluxes associated with the whole SNRs obtained by SRT in comparison with previous results in the literature support the evidence for a possible slight spectral steepening above $\sim$1 GHz for both sources (needing confirmation), which could be related to primary electrons or more likely secondary hadronic electrons cut-offs.

Disentanglement among different theoretical possibilities for explaining the above findings could be provided through the analysis of further high-frequency/high-resolution imaging data. In particular, spatially-resolved, spectral curvature/break measurements could be obtained by coupling $1.5 - 7$ GHz maps with higher-frequency observations, as for instance at $20 - 22$ GHz using SRT's K-band multi-feed receiver (see Loru *et al.*, these proceedings).

References

Abdo, A. A. *et al.* 2010, *Science* 327, 1103
Ackermann, M. *et al.* 2013, *Science* 339, 807
Cardillo, M. *et al.* 2014, *A& A* 565, A74
Cardillo, M., Amato, E., & Blasi, P. 2016, *A& A* 595, 58
Castelletti, G., Dubner, G., Clarke, T., & Kassim, N. E. 2007, *A& A* 471, 537
Castelletti, G., Dubner, G., Clarke, T., & Kassim, N. E. 2011, *A& A* 534, A21
Ellison, D. C., Baring, M. G., & Jones, F. C. 1995, *ApJ* 453, 873
Ellison, D. C., Baring, M. G., & Jones, F. C. 1997, *ApJ* 473, 1029
Giuliani, A. *et al.* 2011, *ApJ* 742, L30
Humensky, B., the VERITAS Collaboration 2015, *ICRC* 34, 875
Lee, S-H., Patnaude, D. J., Raymond, J. C., Nagataki, S., Slane, P. O., & Ellison, D. C. 2015, *ApJ* 806, 71
Sturner, S. J., Skibo, J. G., Dermer, C. D., & Mattox, J. R. 1997, *ApJ* 490, 619